Chinese Journal of Natural Medicines

Multidrug resistance reversal effect of tenacissoside I through impeding EGFR methylation mediated by PRMT1 inhibition

Donghui Liu, Qian Wang, Ruixue Zhang, Ruixin Su, Jiaxin Zhang, Shanshan Liu, Huiying Li, Zhesheng Chen, Yan Zhang, Dexin Kong, Yuling Qiu

Citation: Donghui Liu, Qian Wang, Ruixue Zhang, Ruixin Su, Jiaxin Zhang, Shanshan Liu, Huiying Li, Zhesheng Chen, Yan Zhang, Dexin Kong, Yuling Qiu, Multidrug resistance reversal effect of tenacissoside I through impeding EGFR methylation mediated by PRMT1 inhibition, Chinese Journal of Natural Medicines, 2025, 23(9), 1092−1103. doi: 10.1016/S1875−5364(25)60956−3.

View online: https://doi.org/10.1016/S1875−5364(25)60956−3

Chinese Journal of Natural Medicines 23 (2025) 1092-1103

Contents lists available at ScienceDirect

Chinese Journal of Natural Medicines

journal homepage: www.cjnmcpu.com/

Original article

Multidrug resistance reversal effect of tenacissoside I through impeding EGFR methylation mediated by PRMT1 inhibition

Donghui Liu[a,Δ], Qian Wang[a,Δ], Ruixue Zhang[a], Ruixin Su[a], Jiaxin Zhang[a], Shanshan Liu[a], Huiying Li[a], Zhesheng Chen[b], Yan Zhang[c,*], Dexin Kong[a,*], Yuling Qiu[a,*]

[a] *Tianjin Key Laboratory on Technologies Enabling Development of Clinical Therapeutics and Diagnostics, School of Pharmacy, Tianjin Medical University, Tianjin 300070, China*
[b] *Department of Pharmaceutical Sciences, College of Pharmacy and Health Sciences, St. John's University, Queens, NY 11439, USA*
[c] *School of Traditional Chinese Materia Medica, Shenyang Pharmaceutical University, Shenyang 110016, China*

ARTICLE INFO

Article history:
Received 27 March 2025
Revised 29 April 2025
Accepted 8 May 2025
Available online 20 September 2025

Keywords:
Tenacissoside I
Multidrug resistance reversal effect
PRMT1
Protein methylation
EGFR signaling

ABSTRACT

Cancer multidrug resistance (MDR) impairs the therapeutic efficacy of various chemotherapeutics. Novel approaches, particularly the development of MDR reversal agents, are critically needed to address this challenge. This study demonstrates that tenacissoside I (TI), a compound isolated from *Marsdenia tenacissima* (Roxb.) Wight et Arn, traditionally used in clinical practice as an ethnic medicine for cancer treatment, exhibits significant MDR reversal effects in ABCB1-mediated MDR cancer cells. TI reversed the resistance of SW620/AD300 and KBV200 cells to doxorubicin (DOX) and paclitaxel (PAC) by downregulating ABCB1 expression and reducing ABCB1 drug transport function. Mechanistically, protein arginine methyltransferase 1 (PRMT1), whose expression correlates with poor prognosis and shows positive association with both ABCB1 and EGFR expressions in tumor tissues, was differentially expressed in TI-treated SW620/AD300 cells. SW620/AD300 and KBV200 cells exhibited elevated levels of EGFR asymmetric dimethylarginine (aDMA) and enhanced PRMT1-EGFR interaction compared to their parental cells. Moreover, TI-induced PRMT1 downregulation impaired PRMT1-mediated aDMA of EGFR, PRMT1-EGFR interaction, and EGFR downstream signaling in SW620/AD300 and KBV200 cells. These effects were significantly reversed by PRMT1 overexpression. Additionally, TI demonstrated resistance reversal to PAC in xenograft models without detectable toxicities. This study establishes TI's MDR reversal effect in ABCB1-mediated MDR human cancer cells through inhibition of PRMT1-mediated aDMA of EGFR, suggesting TI's potential as an MDR modulator for improving chemotherapy outcomes.

1. Introduction

Cancer remains a significant global health burden. Statistical data indicate that approximately 19.3 million new cancer cases were documented worldwide in 2020, with cancer-related mortality reaching 10 million [1]. Despite substantial progress in chemotherapy, radiotherapy, targeted therapy, and immunotherapy, the development of multidrug resistance (MDR) continues to compromise the therapeutic efficacy of various chemotherapeutic agents [2, 3]. MDR is characterized by cancer cell resistance to structurally and mechanistically diverse anticancer compounds. The principal mechanisms underlying MDR include drug efflux pump overexpression, enhanced drug metabolism, increased DNA repair capacity, and alterations in apoptotic pathways and tumor microenvironment (TME) [4]. Among these mechanisms, ATP-binding cassette (ABC) membrane transporter-mediated drug efflux has been most extensively investigated [5]. Members of the ABC transporter family, particularly MDR1, encoded by *ABCB1* and known as P-glycoprotein (P-gp), MDR-associated protein-1 (MRP1), encoded by *ABCC1*, and breast cancer resistant proteins (encoded by *ABCG2*), have been shown to induce MDR in cancer cells [3]. Various strategies have been developed to overcome MDR in human cancer. While ABC transporter inhibitors, particularly MDR1/P-gp inhibitors, have shown promise in clinical trials for certain cancers, notably acute myeloid leukemia (AML) [6], their clinical application is limited by severe adverse effects and high toxicity [7]. The exploration of novel MDR reversal drug candidates remains an urgent priority.

Protein arginine methylation represents a significant type of protein post-translational modification (PTM), involved in various complex cellular processes, both physiological and pathological, including protein trafficking, metabolic regulation, and RNA processing [8]. As a crucial PTM enzyme, protein arginine methyltransferases (PRMTs) play an essential role in tumor pathogenesis by catalyzing protein arginine methylation modifications [9]. PRMT1 catalyzes substrate protein arginine methylation by transferring methyl groups of *S*-adenosyl-*L*-methionine (SAM) onto the guanidine nitrogen of protein arginine residues. Based on specific catalytic activities, PRMTs are classified into three

* Corresponding author.
E-mail addresses: zhangyan_929@yeah.net (Y. Zhang); kongdexin@tmu.edu.cn (D. Kong); qiuyuling@tmu.edu.cn (Y. Qiu)
Δ These authors contributed equally to this work.

https://doi.org/10.1016/S1875-5364(25)60956-3

types in mammalian cells. Type I PRMT catalyzes asymmetric dimethylarginine (aDMA) and monomethylarginine (MMA), Type II PRMT generates symmetric DMA (sDMA) and MMA, while Type III PRMT primarily produces MMA. PRMT1 exhibits elevated expression in most solid cancers [10, 11]. Research demonstrates that PRMT1 mediates cellular function by catalyzing methylation of both histone proteins, such as methylating histone H4R3 to form H4R3me2a and promoting transcriptional activation, and significant non-histone proteins, including EGFR, FOXO1, and MRE11 [11-13]. PRMT1's intricate involvement in cancer onset and progression highlights its potential as a promising target in cancer therapy.

Natural products have emerged as potential MDR reversal agents due to their structural diversity and broad biological activities. These compounds overcome tumor cell resistance through various molecular and cellular mechanisms, including regulation of MDR-related proteins and critical signaling pathways [14].

Marsdenia tenacissima is the climbing stem of the Chinese traditional ethnic herb *Marsdenia tenacissima* (Roxb.) Wight et Arn. The commercial preparation of *M. tenacissima*, marketed as Xiao-Ai-Ping injection, consists of its water-soluble extract [15]. This preparation has been approved for cancer treatment in combination with chemotherapy or radiotherapy for several decades [16]. Research has identified that C21 steroid glycosides, tenacissimoside D to J, are abundant in *M. tenacissima*, and constitute its main active ingredients in cancer therapy [17]. Studies indicate that tenacissimoside H inhibits glioblastoma multiforme progression by suppressing PI3K/Akt/mTOR signaling *in vitro* and *in vivo* [18]. Tenacissimoside G enhances the inhibitory activity of 5-FU on human colorectal cancer by arresting cell cycle progression and inducing p53-mediated apoptosis [19], while also reversing resistance to paclitaxel (PAC) by inhibiting Src/PTN/P-gp signaling in ovarian cancer [20]. *M. tenacissima* extract promotes gefitinib accumulation through inhibiting ABCG2 activity in lung cancer treatment [21]. However, the anticancer activity and MDR reversal efficacy of *M. tenacissima*, along with its specific mechanisms, remain unclear.

Tenacissoside I (TI) is a C21 steroid glycoside present at relatively high levels in *M. tenacissima* [22]. This study investigates the MDR reversal effect of TI in cancer chemotherapy, aiming to reveal its potential as an MDR modulator and enhance the clinical outcome of chemotherapy.

2. Materials and methods

2.1. Reagents and cell culture

TI (purity > 98%, HPLC) was obtained from Abphyto Biotech (Chengdu, China). PAC and verapamil (VER) were purchased from Target Molecule Corp (Shanghai, China). Ko143 and cisplatin (CP) were acquired from MCE (Shanghai, China). Doxorubicin (DOX) and Hoechst 33342 were obtained from Meilunbio (Dalian, China). The relevant assay kits and antibodies, along with several conventional methods, are detailed in Supplementary Materials and Table S1.

Human colon cancer cell line SW620, oral epidermoid cancer cell line KB, and their ABCB1-overexpressing drug resistant cell sublines SW620/AD300 (DOX-selected cells) and KBV200 (vincristine-selected cells), another human colon cancer cell line S1 and its ABCG2-overexpressing resistant cell subline S1-M1-80 (mitoxantrone-selected cells) were maintained in RPMI 1640 medium, supplemented with fetal bovine serum (10%), streptomycin (100 $\mu g \cdot mL^{-1}$), and penicillin (100 $U \cdot mL^{-1}$), in a cell incubator (5% CO_2, 37 °C). The drug-resistant cell sublines were cultured in media without chemotherapeutics for at least 2 weeks prior to subsequent experimentation.

2.2. MTT assay

The MTT assay was conducted according to our previous report to evaluate cell viability and MDR reversal effect [23]. Cells were cultured in 96-well plates with 200 μL/well (3×10^4 cells/mL). For cell viability testing, DMSO or TI solution at various concentrations (volume: 0.5 μL) was added, followed by 48 h incubation. For MDR reversal testing, cells pre-treated with TI (at doses maintaining cell viability above 80%) for 2 h were exposed to different concentrations of chemotherapeutic agents for 48 h. Subsequently, cells were incubated with MTT solution (5 $mg \cdot mL^{-1}$, 4 h, 37 °C) and analyzed using an iMark microplate reader (BIO-RAD, USA). The half-maximal inhibitory concentration (IC_{50}) of each chemotherapeutic was determined, and the corresponding resistance fold (RF) was calculated. VER served as a positive control and CP as a negative control.

2.3. Western blot

Western blot analysis procedures in this study were consistent with our previous publication [24]. The detailed experimental protocol is available in Supplementary Materials. Original Western blot membrane bands are presented in Figures S1-S12.

2.4. DOX accumulation assay by flow cytometry

Intracellular DOX accumulation in ABCB1-mediated MDR cells was analyzed using flow cytometry, as previously reported [23]. Sensitive cell lines (SW620 and KB) and drug-resistant cell sublines (SW620/AD300 and KBV200) were seeded in 6-well plates (2×10^5 cells/well) and pre-treated with vehicle control, TI (10, 25 $\mu mol \cdot L^{-1}$), or VER (10 $\mu mol \cdot L^{-1}$) for 2 h, followed by DOX co-treatment for an additional 2 h. After harvesting, cells underwent flow cytometry analysis (Accuri C6, BD Biosciences, San Jose, CA, USA) to assess intracellular DOX fluorescence intensity.

2.5. DOX efflux assay by flow cytometry

Drug efflux analysis of ABCB1-mediated MDR cells was performed using Flow cytometry, as previously described [23]. Cells were pre-incubated with DOX (37 °C, for 2 h), washed with ice-cold PBS, and treated with control, TI (10, 25 $\mu mol \cdot L^{-1}$) or VER (10 $\mu mol \cdot L^{-1}$) in a fresh medium for 0, 30, 60, 120 min. Intracellular DOX fluorescence intensity was measured using flow cytometry (Accuri C6, BD Biosciences, San Jose, CA, USA).

2.6. Quantitative real-time polymerase chain reaction (qRT-PCR)

QRT-PCR procedure followed previously described methods [25]. The specific experimental protocol and primer list are provided in Supplementary Materials and Table S2.

2.7. Proteome analysis

SW620/AD300 cells (2×10^5 per well, 2 mL/well in a six-well plate) were incubated with either DMSO (vehicle control) or TI (25 $\mu mol \cdot L^{-1}$) for 48 h. The collected cells underwent proteome analysis at PTM Bio (Hangzhou, Zhejiang, China). Differential proteomic analysis utilized the limma (v.3.58.1) package [26]. Differentially expressed proteins (DEPs) were visualized in a volcano plot using the ggplot2 (v.3.5.1) and ggrepel (v.0.9.5) packages (P-value < 0.05). Heatmaps were generated using the pheatmap (v.1.0.12) package. DEPs underwent functional enrichment analysis through mapping to the Gene Ontology (GO) database *via* the ClueGO plugin in Cytoscape software. Statistical significance was determined using a two-tailed hypergeometric test, with p-values adjusted for multiple comparisons using the Benjamini-

Hochberg method (adjusted P-value < 0.05).

2.8. PRMT1 overexpression

PRMT1 overexpression in experimental cells was achieved using a lentiviral vector (GV492). The lentiviral expression vector (GV492) was obtained from Genechem (Shanghai, China). Stable cell lines were selected using puromycin, and overexpression was confirmed through Western blot and qRT-PCR analysis.

2.9. Xenograft model

Male BALB/c nude mice (5 weeks old) were obtained from The Animal Center of Tianjin Medical University and maintained under conditions consistent with our previously reported protocols [25, 26]. All animal procedures were conducted according to the Laboratory Animal Management and Use Committee of Tianjin Medical University guidelines (No. TMUaMEC 2024033, date: Jan 8th, 2025). Subcutaneous xenograft tumors were established by injecting SW620/AD300 cells (1×10^7 cells/mouse in 100 μL PBS) into the right flank. When tumor volumes reached approximately 100 mm^3 (volume = length × $width^2/2$), the animals were randomly assigned to four groups: (1) control group (i.p., q2d); (2) TI treatment group (i.p., 20 $mg \cdot kg^{-1}$, q2d); (3) PAC treatment group (i.p., 10 $mg \cdot kg^{-1}$, q2d); (4) TI combined with PAC treatment group (i.p., 20 $mg \cdot kg^{-1}$ TI administered 1 h before 10 $mg \cdot kg^{-1}$ PAC injection, q2d). Tumor size measurements were taken every two days throughout the experimental period. Subsequently, mice were humanely euthanized, and tumor tissues were surgically excised for further evaluations.

2.10. Immunoprecipitation (IP) and Co-IP

IP and Co-IP procedures were performed following established protocols [24]. Cells cultured in 6-well plates (2×10^5 cells/well) received treatment with 25 $\mu mol \cdot L^{-1}$ TI for 48 h, followed by lysis with ice-cold cell lysis buffer for 30 min at 4 °C. The lysates were separated into two portions. One portion underwent IP analysis, using normal rabbit immunoglobulin G (IgG) as a control. The second portion was analyzed by immunoblotting as input.

2.11. Statistics

Quantitative results represent the mean of three replicates (mean ± standard deviation) per experiment. Statistical analyses were performed using GraphPad Prism software (version 8.0; GraphPad Software, La Jolla, CA), employing either one-way ANOVA or Student's t-test. Statistical significance was defined as $P < 0.05$.

3. Results

3.1. MDR reversal of tenacissoside I in ABCB1-overexpressing human cancer cells

Fig. 1A depicts TI's chemical structure. SW620, KB, and their ABCB1-overexpressing drug resistance cell lines SW620/AD300 and KBV200 served as cell models. The drug resistance characteristics of MDR cell lines and TI's impact on cell viability were assessed through the MTT assay. SW620/AD300 and KBV200 cells demonstrated substantial drug resistance to DOX compared to parental cells, with resistance fold (RF) values of 56.66 and 408.13, respectively (Table S3). Cell viability tests revealed that TI exhibited minimal cytotoxicity, with cell growth inhibition rates remaining below 20% at concentrations under 80 $\mu mol \cdot L^{-1}$ across all selected cell models (Fig. 1B). Consequently, TI concentrations of 10 and 25 $\mu mol \cdot L^{-1}$ were selected for subsequent MDR reversal investigation. To evaluate TI's MDR reversal effect, parental cells and their MDR cells pre-treated with TI or VER for 2 h were exposed to DOX, PAC, or CP for 48 h. VER, a potent ABCB1 inhibitor, served as a positive control, while CP functioned as a negative control. CP resistance involves multiple mechanisms, including altered drug uptake/efflux, enhanced DNA repair capacity, glutathione conjugation, and apoptosis evasion. CP is not an ABCB1 substrate. Results indicated that TI treatment, similar to VER, significantly reduced the IC_{50} values of DOX and PAC in SW620/AD300 and KBV200 cells, while maintaining unchanged IC_{50} values in parental cells (Fig 1C). Correspondingly, significant decreases in RF values for DOX and PAC were observed in the TI pre-treated group (Fig 1D), declining from 57.11 and 1709.74 in the control group to 2.00 and 354.53 in the TI (25 $\mu mol \cdot L^{-1}$) pretreatment group for SW620/AD300, and from 398.24 and 20.55 to 20.64 and 2.46 for KBV200, respectively. RF values for CP remained constant, demonstrating TI's MDR reversal effect in ABCB1-overexpressing cells. These results indicate that TI effectively reverses ABCB1-mediated MDR in cancer cells.

3.2. ABCB1 drug transport regulation of TI in ABCB1-overexpressing human cancer cells

Given that ABC transporter family members ABCB1 and ABCG2 are extensively involved in cancer MDR [3, 5], this study evaluated the drug reversal effect of TI in mitoxantrone-selected ABCG2-overexpressing cell line, S1-M1-80. Results in Fig. 2A and Fig. S13 demonstrated that, compared with Ko143, an ABCG2 inhibitor serving as a positive control, TI exhibited a negligible MDR reversal effect in S1-M1-80 cells, suggesting TI functions specifically as an ABCB1-mediated MDR reversal agent. To elucidate the mechanism underlying TI's reversal effect in ABCB1-mediated MDR, the influence of TI on ABCB1 expression and drug transport activity was analyzed. The investigation revealed that ABCB1 protein levels corresponded with mRNA levels, showing a modest reduction in SW620/AD300 and KBV200 cells following TI treatment (Figs. 2B and 2C). Immunofluorescence (IF) analysis confirmed a substantial decrease in ABCB1 fluorescence intensity in TI-treated groups compared to controls in MDR cell lines. Additionally, ABCB1 membrane abundance decreased significantly with TI treatment, suggesting a potential reduction in drug transport capacity (Fig. 2D).

The intracellular concentration of chemotherapy drugs is partially determined by the ABC transporters' drug transport function and influences therapeutic efficacy. Therefore, the study examined intracellular dynamics of chemotherapy drugs following TI treatment. Flow cytometry quantitatively assessed DOX accumulation and efflux in both parental and MDR cell lines after TI treatment. Results in Fig. 2E demonstrated that TI significantly inhibited DOX efflux in SW620/AD300 and KBV200 cells, while showing no detectable changes in their parental cells. At 120 minutes, the DOX efflux rate in SW620/AD300 cells decreased from 80.04% in controls to 62.15% with high-dose TI treatment (25 $\mu mol \cdot L^{-1}$), comparable to the positive control (VER). In KBV200 cells, the efflux percentage decreased from 80.86% to 48.43% following TI treatment (25 $\mu mol \cdot L^{-1}$). TI showed no significant effect on DOX efflux in parental SW620 and KB cells, where drug efflux rates remained at 20%–30% (Fig. 2E). Quantification of intracellular drug accumulation revealed dose-dependent increases in DOX accumulation in TI-treated SW620/AD300 and KBV200 cells compared to controls, while showing minimal impact on parental cells (Fig. 2F). These findings indicate that TI enhances intracellular retention of chemotherapeutics by modulating ABCB1's drug transport function, thereby contributing to drug resistance reversal in ABCB1-mediated MDR cancer cells.

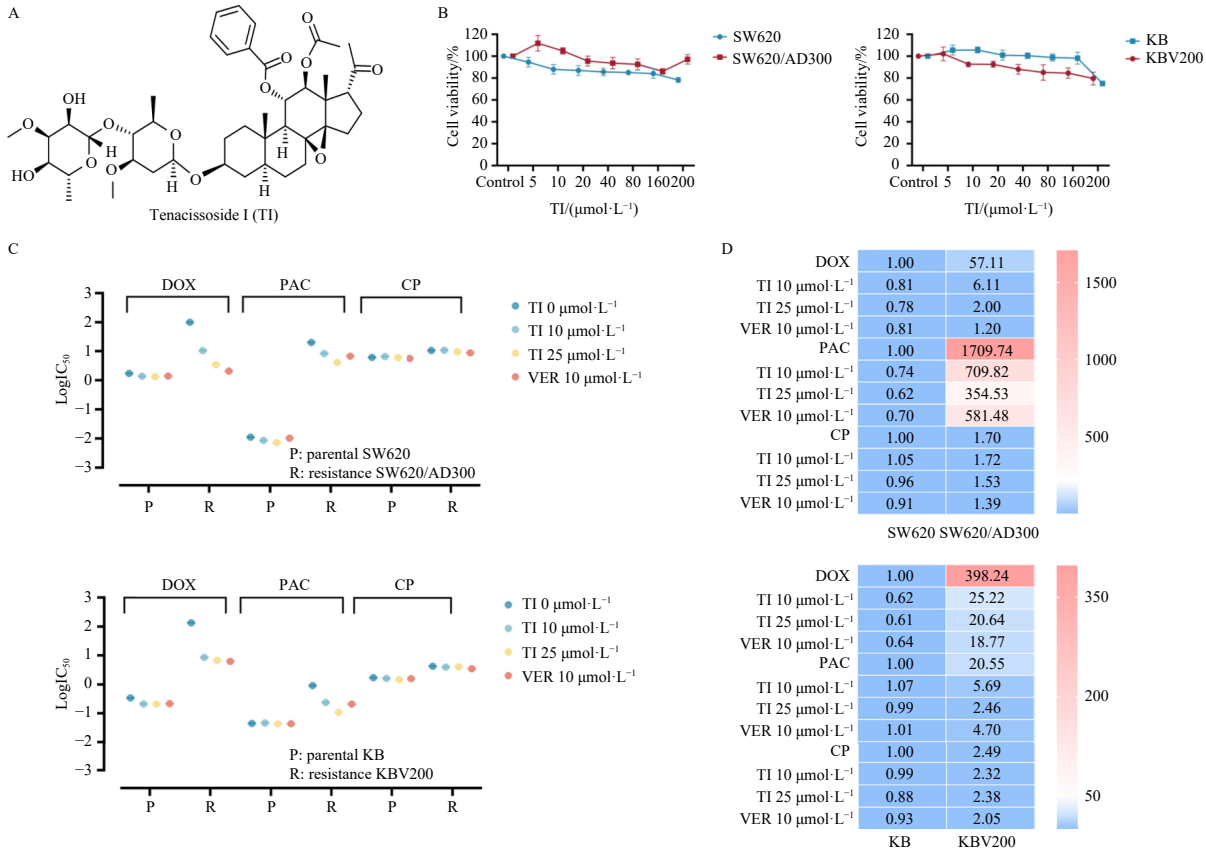

Fig. 1 Reversal of drug resistance by TI in ABCB1-mediated MDR cancer cells. (A) Chemical structure of TI. (B) Cell viability of SW620, SW620/AD300 (DOX selected ABCB1-overexpressing cell subline), KB, and KBV200 (vincristine selected ABCB1-overexpressing cell subline) cells assayed by MTT after 48-h exposure to TI. (C) LogIC_{50} values of DOX, PAC, and CP in SW620, SW620/AD300, KB, and KBV200 cells with or without 2-h pre-treatment with TI (10, 25 μmol·L^{-1}). VER was used as a positive control for drug resistance reversal. (D) RF, calculated from IC_{50} values of the indicated chemotherapeutics in the respective cell models before and after TI exposure, is presented as a heatmap. Data are presented as mean ± SD (n = 3 independent experiments).

3.3. PRMT1-mediated asymmetric dimethylation of EGFR is closely involved in MDR in ABCB1-overexpressing human cancer cells

To elucidate the regulatory mechanism underlying TI-mediated reversal of MDR in ABCB1-overexpressing cancer cells, proteomic analysis was conducted on SW620/AD300 cells after 48 h treatment with or without TI (25 μmol·L^{-1}) to compare protein profiles. The results in Figs. 3A and 3B revealed 2436 significantly DEPs in TI-treated SW620/AD300 cells, comprising 1248 upregulated and 1188 downregulated proteins. ClueGO enrichment analysis of downregulated proteins demonstrated that biological processes, including ABC-type transporter activity, signal transduction and protein complex oligomerization, and key factors such as PRMT1, were predicted to be involved in TI's effect on SW620/AD300 cells (Fig. 3C). As PRMT1 is the predominant aDMA methyltransferase strongly associated with various cellular processes, including tumorigenesis [9, 11, 27], analysis of PRMT1 expression in multiple tumor tissues and normal tissues in the TCGA database revealed significantly elevated PRMT1 expression in multiple tumor tissues compared to adjacent non-tumor tissues (Fig. 3D). Moreover, survival analysis based on TCGA-colon adenocarcinoma (COAD) dataset indicated that colon cancer patients with high PRMT1 expression exhibited significantly worse survival probabilities compared to those with low PRMT1 levels (P = 1.053e-03), confirming PRMT1's carcinogenic role (Fig. 3E).

Correlation analysis demonstrated that PRMT1 expression positively correlated with both ABCB1 and EGFR expressions in tumor tissues of colon cancer patients from the TCGA-COAD dataset (Figs. 3F and 3G). Previous studies have indicated that PRMT1-mediated EGFR methylation represents its regulation of EGFR function [28]. Additionally, ABCB1 is reportedly activated by EGFR [29]. Based on these findings, we hypothesized that PRMT1-mediated EGFR methylation might be critically involved in cancer MDR progression. Examination of EGFR methylation status and interactions between EGFR and PRMT1 in ABCB1-overexpressing MDR cells and their parental cells revealed that the aDMA level of EGFR was significantly increased in SW620/AD300 and KBV200 cells compared to their parental counterparts, SW620 and KB (Fig. 3H). Co-IP assays further confirmed stronger interactions between PRMT1 and EGFR in SW620/AD300 and KBV200 cells than in parental cells (Fig. 3I). These findings suggest that PRMT1 may serve as a key therapeutic target in addressing cancer MDR, and PRMT1-mediated aDMA of EGFR is closely involved in MDR formation in ABCB1-overexpressing human cancer cells.

3.4. TI inhibits EGFR signaling through impairing PRMT1-mediated asymmetric dimethylation of EGFR

Following the preliminary evidence that PRMT1-mediated aDMA of EGFR contributes to cancer MDR formation, this study investigated whether TI's MDR reversal efficacy relates to PRMT1-mediated aDMA of EGFR. Initial examination of PRMT1 expression in SW620/AD300 and KBV200 cells exposed to TI revealed dose-dependent and time-dependent reductions in PRMT1 protein expression in both MDR cell lines (Figs. 4A and 4B). To elucidate the underlying mechanism, SW620/AD300 and KBV200 cells were treated with TI (25 μmol·L^{-1}, 48 h) and analyzed *via* IP to assess EGFR aDMA modification. Co-IP analysis evaluated EGFR-PRMT1 interactions. As demonstrated in Fig. 4C, TI treatment significantly decreased aDMA modification while maintain-

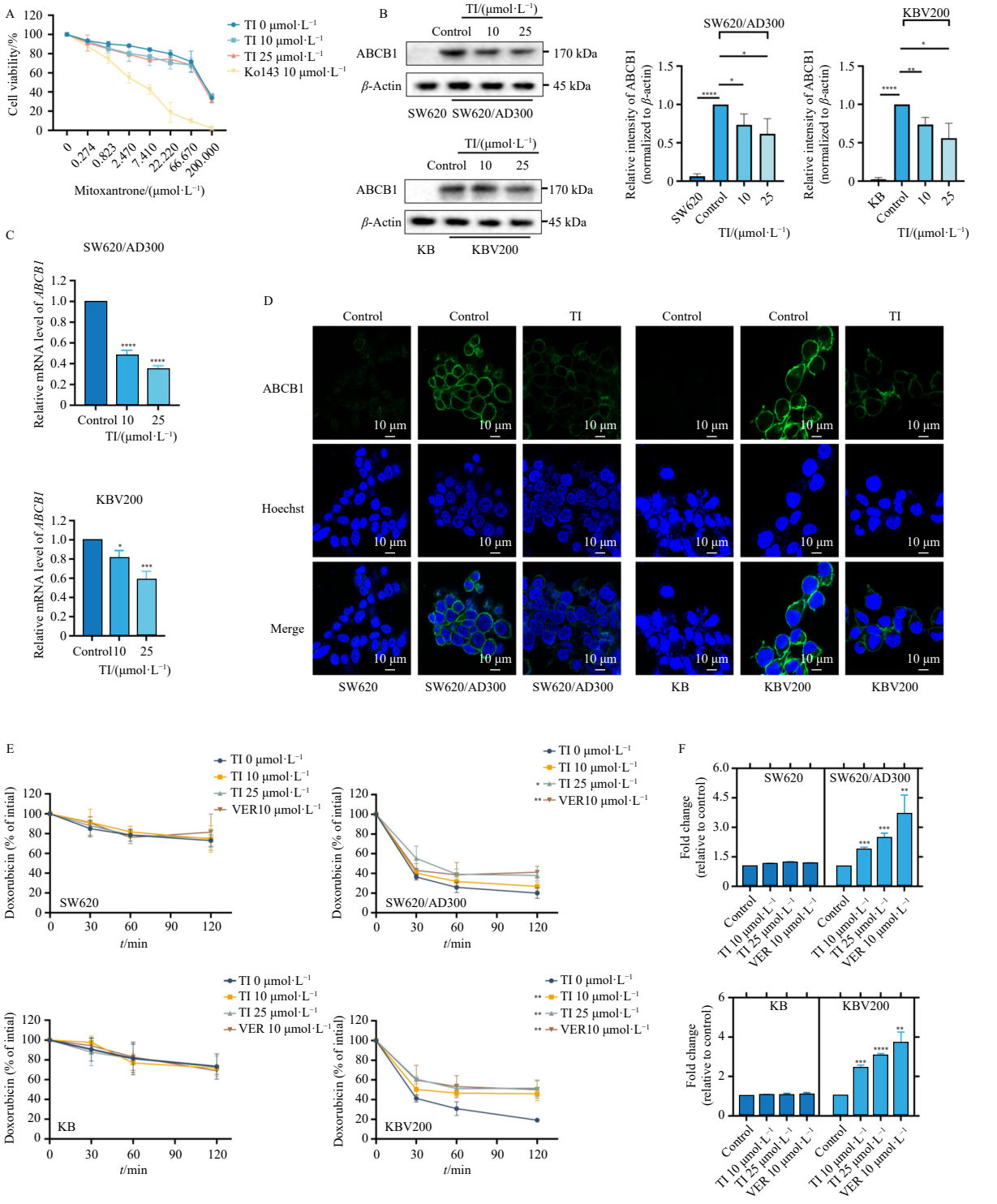

Fig. 2 TI inhibited ABCB1 expression and regulated its drug transport function. (A) Drug reversal effect of TI in S1-M1-80 cells (mitoxantrone-selected ABCG2-overexpressing cell subline) evaluated by MTT assay. (B–C) Effects of TI on ABCB1 expression at the protein level (B, Western blot) and mRNA level (C, qRT-PCR). (D) IF analysis of ABCB1 subcellular localization (scale bar, 10 μm). (E–F) Quantitative analysis of DOX efflux (E) and accumulation (F) in SW620, SW620/AD300, KB, and KBV200 cells following treatment with TI or verapamil (VER, positive control), measured by flow cytometry. Data are presented as mean ± SD (n = 3 independent experiments). $^{*}P < 0.05$, $^{**}P < 0.01$, $^{***}P < 0.001$, $^{****}P < 0.0001$.

ing MMA levels of EGFR in both cell lines. Additionally, EGFR-PRMT1 interactions were notably diminished upon TI exposure in both MDR cell lines (Fig. 4D). These findings support the initial hypothesis and indicate that TI inhibits both PRMT1 and PRMT1-mediated aDMA of EGFR in SW620/AD300 and KBV200 cells. Since EGFR methylation influences its activity and downstream signaling, Western blot analysis of EGFR signaling effectors revealed that TI treatment reduced phosphorylation of EGFR (p-EGFR, Tyr1068) and key downstream effectors Erk and Akt in both cell lines (Figs. 4E–4G), demonstrating EGFR signaling inhibition. These results suggest that TI inhibits EGFR signaling through impairment of PRMT1-mediated aDMA of EGFR in ABCB1-overexpressing human cancer cells.

3.5. TI reverses drug resistance probably through inhibiting PRMT1-mediated asymmetric dimethylation of EGFR

Given PRMT1's potential role in TI's drug resistance reversal

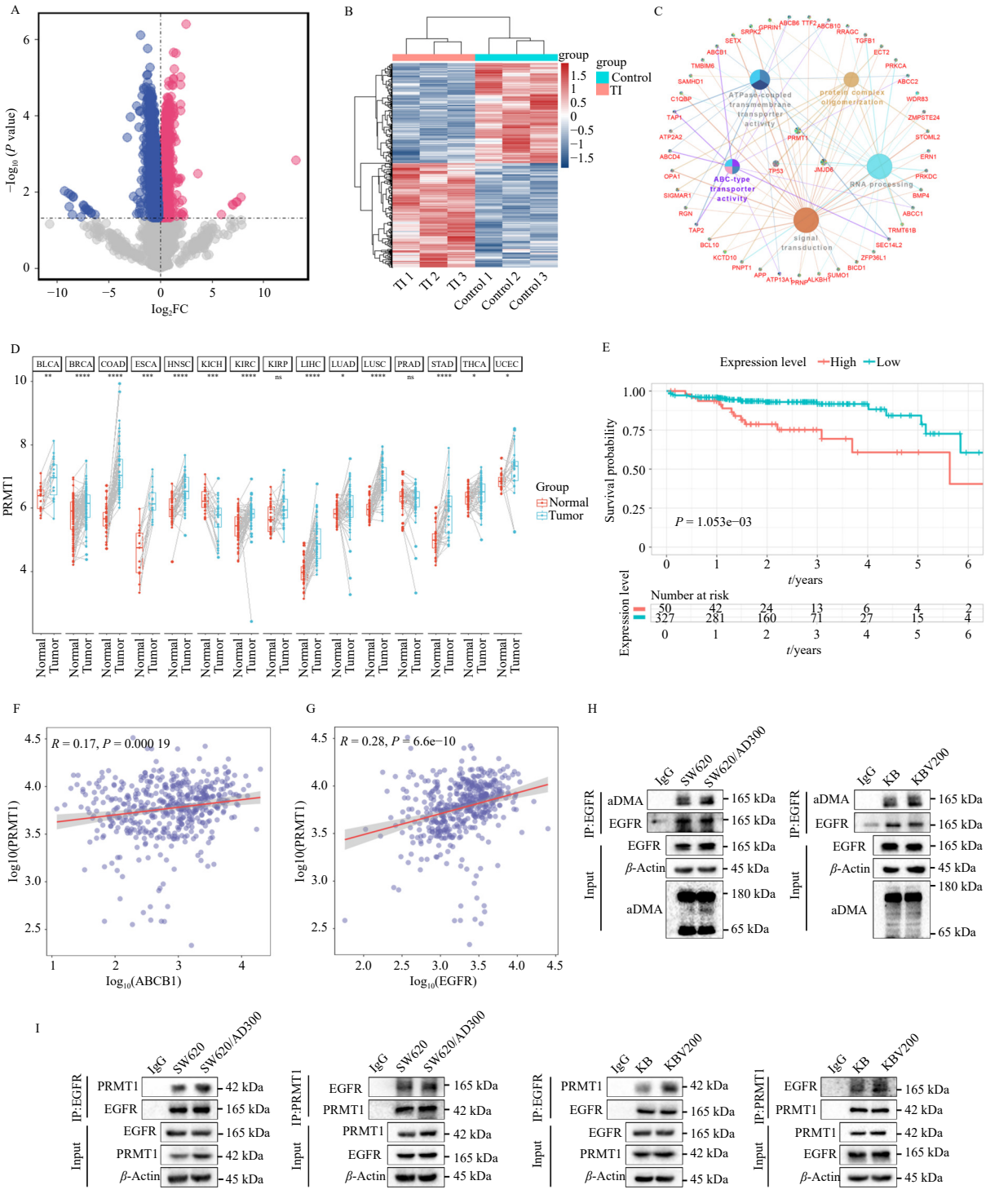

Fig. 3 PRMT1-mediated EGFR asymmetric dimethylation contributed to TI-induced drug resistance reversal. (A–B) Proteomic profiling of SW620/AD300 cells exposed to DMSO or TI (25 μmol·L^{-1}) for 48 h (n = 3). DEPs were displayed in a volcano plot (A) and hierarchical clustering heatmap (B). Significance threshold: P < 0.05; values are $\log_2$fold change ($\log_2$FC). (C) ClueGO enrichment analysis of biological processes associated with downregulated proteins identified in (A). (D) PRMT1 expression levels in various tumor tissues compared with adjacent normal tissues from the TCGA database. (E) Kaplan-Meier survival analysis of colon cancer patients stratified by high versus low PRMT1 expression based on the TCGA-COAD dataset. (F–G) Correlation scatterplots depicting associations between PRMT1 expression and ABCB1 (F) or EGFR (G) expression in colon cancer tumor samples from TCGA-COAD. Spearman correlation analysis revealed significant positive correlations: PRMT1 *vs* ABCB1 (R = 0.17, P = 0.00019) and PRMT1 *vs* EGFR (R = 0.28, P = 6.6e−10). (H) Evaluation of EGFR asymmetric dimethylation in SW620, SW620/AD300, KB, and KBV200 cells by immunoprecipitation (IP). Partial total lysates were used as input and analyzed by Western blot. (I) Interactions between PRMT1 and EGFR in SW620, SW620/AD300, KB, and KBV200 cells by co-immunoprecipitation (Co-IP). Partial total lysates were were used as input and analyzed by Western blot.

effect in ABCB1-overexpressing MDR cells, PRMT1 was overexpressed in SW620/AD300 and KBV200 cells, and TI's reversal effect was evaluated in PRMT1-overexpressing SW620/AD300^{PRMT1} and KBV200^{PRMT1} cells. PRMT1 overexpression was confirmed through Western blot (Fig. 5A). MTT assays assessed TI's efficacy in reversing drug resistance to DOX or PAC in both standard and PRMT1-overexpressing cell lines. The results demonstrated that the MDR reversal effect of TI was significantly reduced in SW620/AD300^{PRMT1} and KBV200^{PRMT1} cells compared to their standard counterparts (Fig. 5B), suggesting that PRMT1 overexpression partially counteracts TI's drug resistance reversal effect in ABCB1-overexpressing human cancer cells.

The aDMA modification of EGFR and the interactions between PRMT1 and EGFR in SW620/AD300 and KBV200 cells

exposed to TI (25 μmol·L^{-1}) for 48 h before or after PRMT1 overexpression were analyzed. Results in Fig. 5C demonstrated that TI-induced reduction of EGFR methylation in SW620/AD300 and KBV200 cells was significantly reversed in the PRMT1-overexpressing cell lines. Similarly, the diminished PRMT1 and EGFR interaction caused by TI in SW620/AD300 and KBV200 cells was

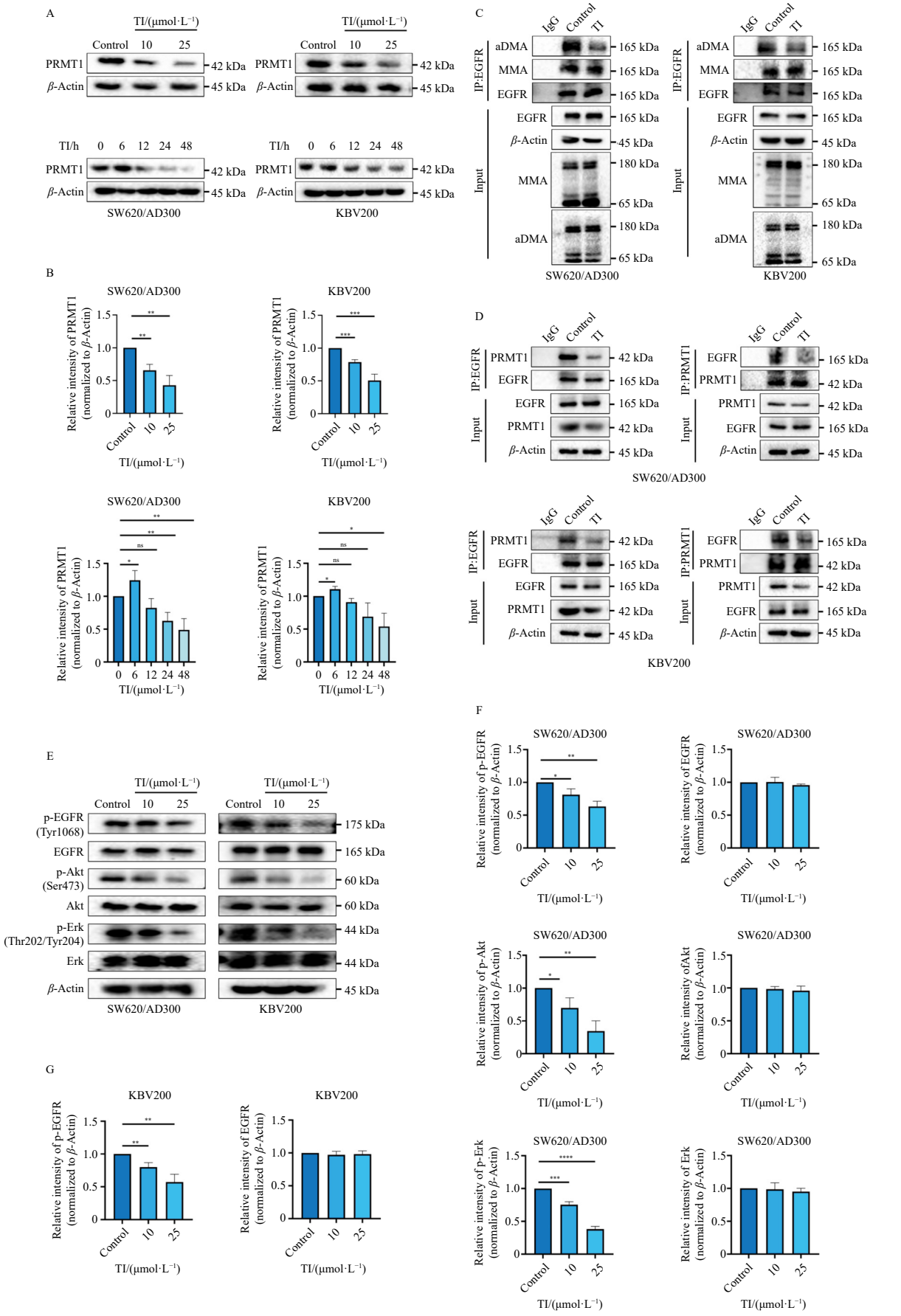

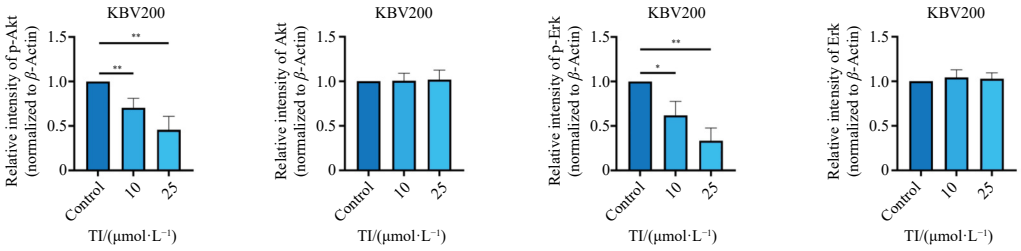

Fig. 4 EGFR signaling suppression by TI through inhibiting PRMT1-mediated asymmetric dimethylation of EGFR. (A, B) PRMT1 expression in SW620/AD300 and KBV200 cells following TI treatment at the indicated concentrations and durations, assessed by Western blot. (C) Evaluation of EGFR asymmetric dimethylation in SW620/AD300 and KBV200 cells treated with or without TI for 48 h, analyzed by immunoprecipitation (IP). Partial total lysates served as input. (D) Interaction between EGFR and PRMT1 in SW620/AD300 and KBV200 cells analyzed by co-immunoprecipitation (Co-IP), with partial total lysates used as input. (E-G) Western blot analysis of EGFR downstream signaling pathways. Data are presented as mean ± SD (n = 3 independent experiments). $^{*}P < 0.05$, $^{**}P < 0.01$, $^{***}P < 0.001$, $^{****}P < 0.0001$, ns, no statistical significance.

reversed following PRMT1 overexpression (Fig. 5D). Additionally, p-EGFR (Tyr1068), p-Akt (Ser473), and p-Erk (Thr202/Tyr204) in SW620/AD300 and KBV200 cells in response to TI (25 μmol·L^{-1}) before or after PRMT1 overexpression were evaluated by Western blot. Results in Figs. 5E–5G indicated that TI significantly downregulated PRMT1, p-EGFR (Tyr1068), p-Akt (Ser473), and p-Erk (Thr202/Tyr204) in SW620/AD300 and KBV200 cells, while this inhibition was notably reversed by PRMT1 overexpression, suggesting that PRMT1 overexpression may restore activation of the EGFR signaling pathway inhibited by TI, thereby counteracting TI's drug resistance reversal effect in ABCB1-overexpressing human cancer cells. These findings indicate that PRMT1-mediated aDMA of EGFR plays a crucial role in TI-induced drug resistance reversal effect in ABCB1-overexpressing human cancer cells.

3.6. Drug resistance reversal of TI in the xenograft model

To verify the *in vivo* drug resistance reversal effect of TI in ABCB1-mediated MDR, xenograft models were established by subcutaneously inoculating SW620/AD300 cells into nude mice. Tumor growth and body weight were monitored to assess the

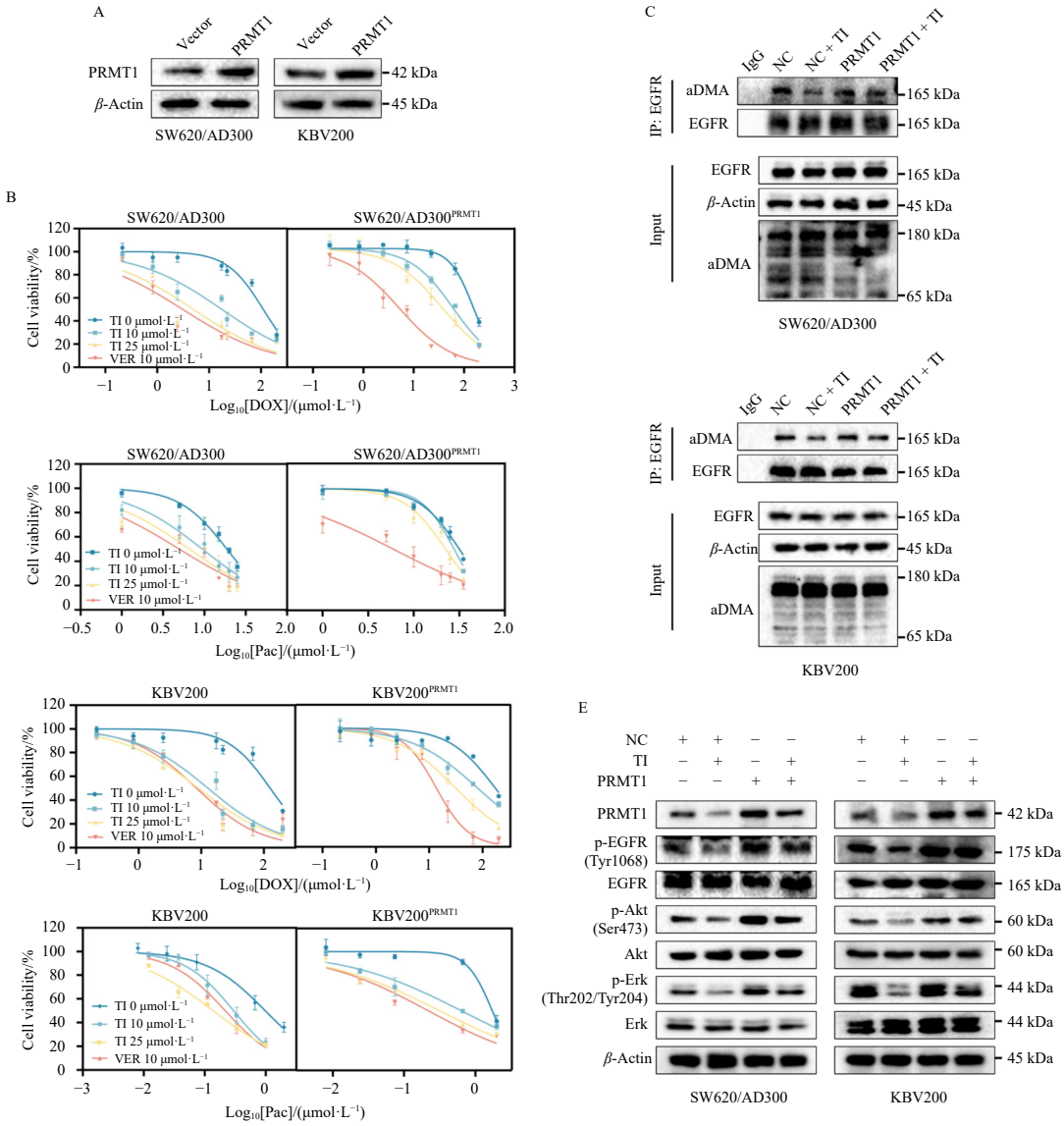

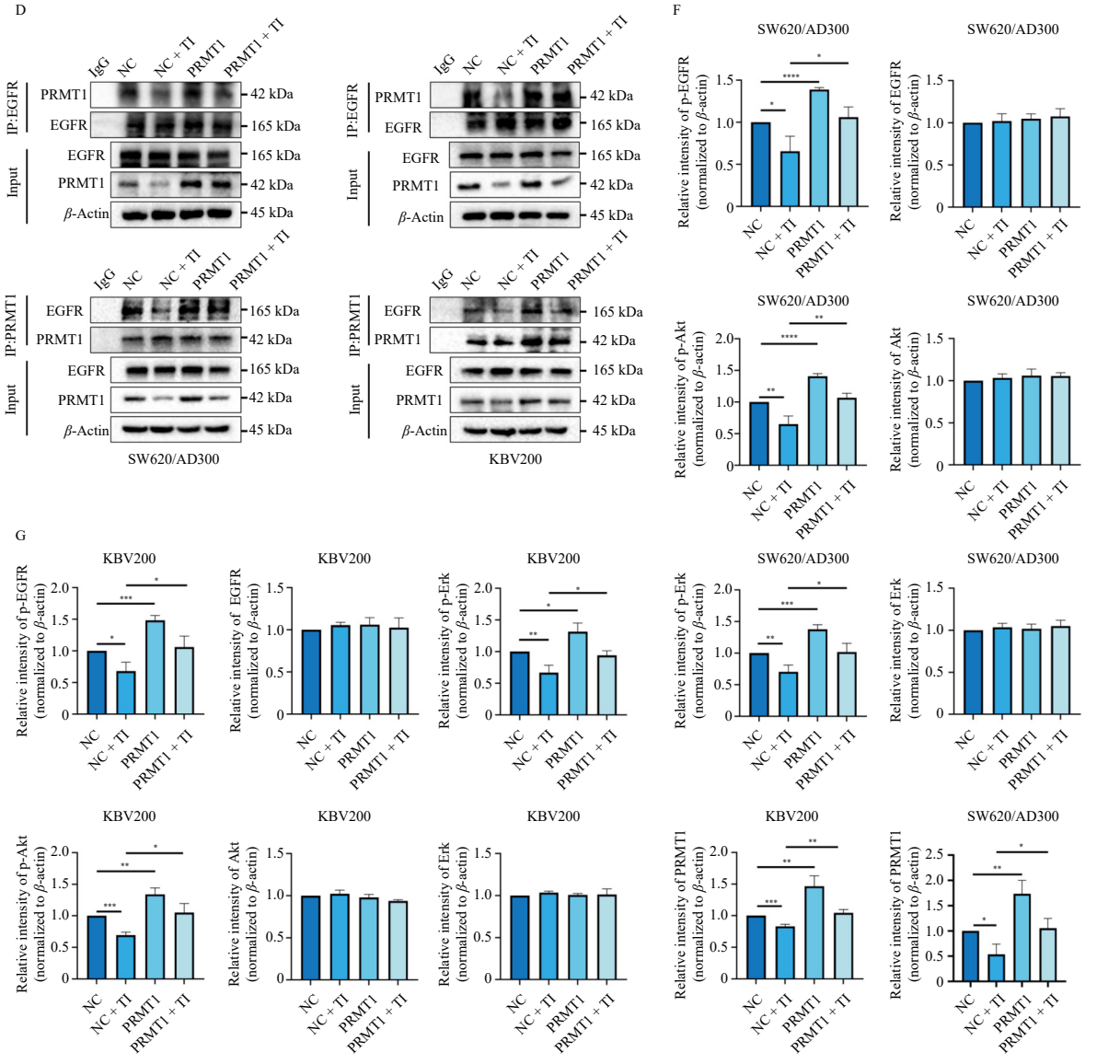

Fig. 5 Impairment of PRMT1-mediated EGFR asymmetric dimethylation contributed to TI-induced drug resistance reversal. (A) Validation of stable PRMT1-overexpressing cell lines SW620/AD300^{PRMT1} and KBV200^{PRMT1}. (B) MTT assay evaluating the effect of TI on reversing drug resistance of SW620/AD300, KBV200, SW620/AD300^{PRMT1}, and KBV200^{PRMT1} cells to DOX and PAC. (C) IP analysis of EGFR asymmetric dimethylation in SW620/AD300 and KBV200 cells treated with or without TI for 48 h, before or after PRMT1 overexpression. Partial total lysates served as input and were analyzed by Western blot. (D) Co-IP analysis of TI's effect on EGFR–PRMT1 interactions in SW620/AD300 and KBV200 cells with or without PRMT1 overexpression. Partial total lysates were analyzed by Western blot as input. (E–G) Western blot analysis of TI's impact on the EGFR signaling pathway in SW620/AD300 and KBV200 cells with or without PRMT1 overexpression. Data are presented as mean ± SD (n = 3 independent experiments). $^{*}P < 0.05$, $^{**}P < 0.01$, $^{***}P < 0.001$, $^{****}P < 0.0001$.

MDR reversal efficacy of TI on SW620/AD300 cells to PAC. As shown in Figs. 6A and 6B, PAC exhibited modest tumor growth inhibition in xenograft models. However, TI at the dose of 20 mg·kg^{-1} significantly enhanced PAC's growth inhibition in xenograft models, demonstrating the drug reversal efficacy of TI. After 14 days of drug administration, the dissected subcutaneous tumor tissues from mice in different groups were weighed, and the results confirmed that the combination of TI plus PAC produced significantly lower tumor weight compared to PAC monotherapy (Fig. 6C). Notably, no changes in mice body weight were observed across all experimental groups during the entire experimental period (Fig. 6D). Additionally, liver and kidney functions (plasma biochemical evaluation) of mice in different treatment groups remained stable, with alanine aminotransferase (ALT), aspartate aminotransferse (AST), creatinine (CREA) and blood urea nitrogen (BUN) maintaining normal levels (Fig. 6E). Hematoxylin and eosin (H&E) analysis revealed minimal toxicity of the combination regimen (Fig. 6F). Furthermore, PRMT1, p-EGFR (Tyr1068), and ABCB1 levels in tumor tissues were downregulated by the TI and PAC combination regimen, compared with PAC monotherapy (Fig. 6G). aDMA modification of EGFR in mouse tumor tissues was also reduced by TI and PAC co-administration, compared with PAC administration alone (Fig. S14). These findings demonstrate that TI effectively reverses ABCB1-mediated MDR while exhibiting minimal toxicity in xenograft models.

4. Discussion

Cancer MDR remains a significant obstacle limiting the clinical efficacy of various chemotherapeutic agents against cancers [2,5]. Multiple mechanisms, including decreased intracellular drug retention due to impaired drug absorption or enhanced drug efflux, abnormal expression of drug transporters, drug target mutations, and metabolic drug inactivation, enable cancer cells to evade chemotherapy and develop MDR [30]. Furthermore, the TME may contribute to MDR by inhibiting drug penetration [31]. These processes are governed by numerous distinct mechanisms [30]. The primary challenges in MDR-related cancer treatment for the com-

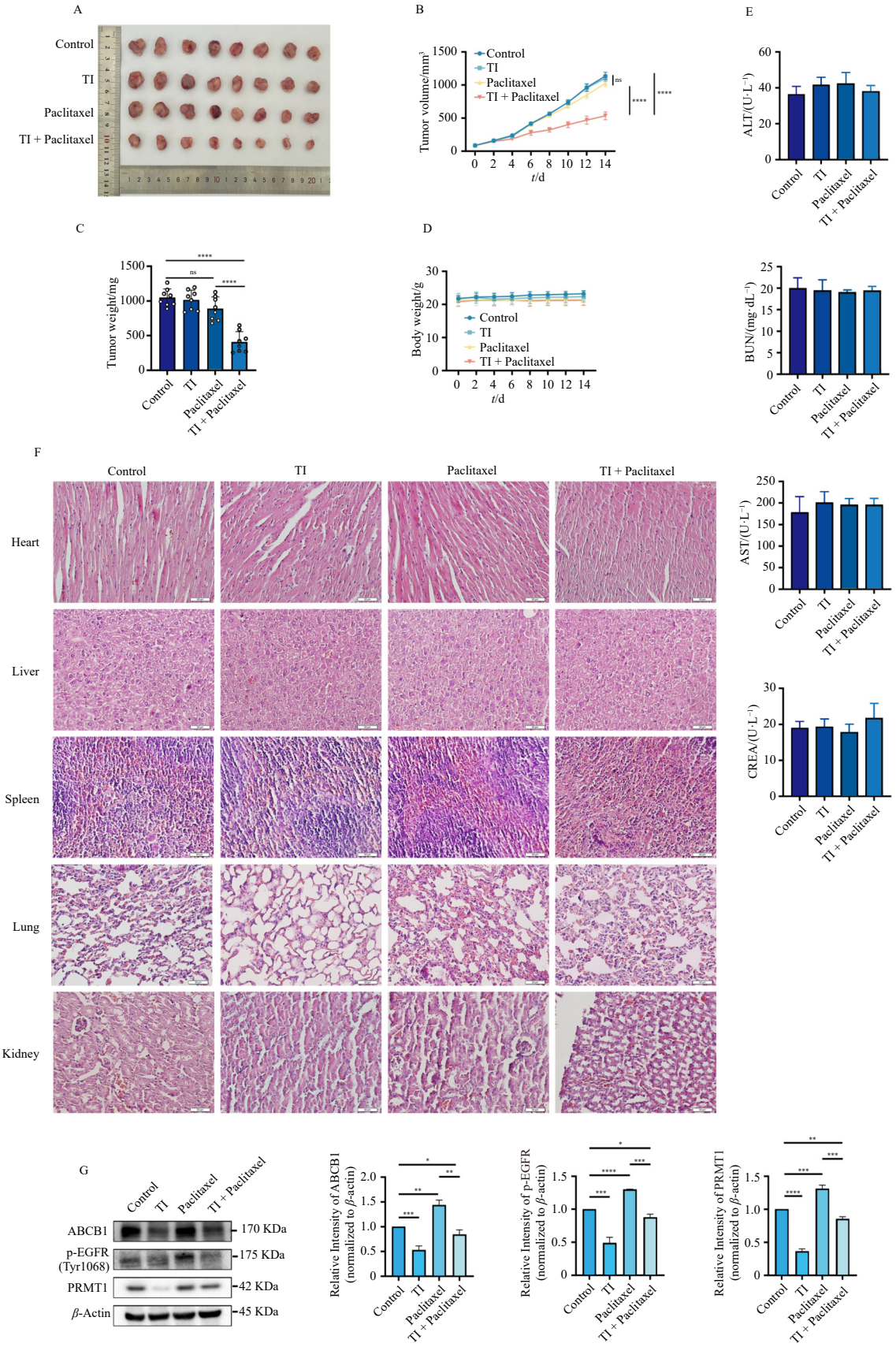

Fig. 6 TI increased paclitaxel sensitivity in the xenograft model. (A–C) Subcutaneous xenograft tumors were established in mice using SW620/AD300 cells and divided into four groups: Control (i.p., q2d), TI (i.p., 20 mg·kg^{-1}, q2d), PAC group (i.p., 10 mg·kg^{-1}, q2d), and TI + PAC groups (i.p., 20 mg·kg^{-1} TI for 1 h before 10 mg·kg^{-1} paclitaxel injection, q2d). Representative images of dissected tumors at the experimental endpoint (A), tumor volume (B), and tumor weight (C) measurements (n = 8). (D) Body weight measurements of mice across treatment groups during the study period (n = 8). (E) Plasma biochemical assays assessing liver and kidney function, including alanine aminotransferase (ALT), aspartate aminotransferase (AST), creatinine (CREA), and blood urea nitrogen (BUN). (F) Hematoxylin and eosin (H&E) staining of major organs, including the heart, liver, spleen, lung, and kidney (scale bar, 50 μm). (G) Western blot analysis of PRMT1, p-EGFR (Tyr1068), and ABCB1 levels in tumor tissues of mice from the indicated groups. Data are presented as mean ± SD (n = 3 independent experiments). $^{*}P < 0.05$, $^{**}P < 0.01$, $^{***}P < 0.001$, $^{****}P < 0.0001$, ns, no statistical significance.

ing years include understanding specific resistance mechanisms, identifying crucial molecular targets and signaling pathways, and utilizing these findings to develop more effective therapeutic strategies. Consequently, future prospects for MDR treatment depend on multifaceted approaches, including novel anti-MDR drug development, innovative diagnostic methods, and optimized treatment protocols, thereby providing more precise and effective therapeutic options [32]. This study demonstrates that TI, a C21 steroid compound, effectively reverses drug resistance in ABCB1-mediated MDR cancer cells with minimal toxicity, highlighting its potential as an MDR reversal drug candidate.

Arginine methylation is primarily catalyzed by PRMTs. These enzymes catalyze the methylation of histones, transcription factors, and various regulatory proteins, resulting in modified gene expression patterns, epigenetic changes, and altered cell survival and growth. Abnormal expression and activity of PRMTs contribute to cancer initiation and progression [33]. The mechanism by which PRMTs impact cancer is multifaceted. PRMT5 promotes colorectal cancer metastasis through SMAD4 methylation and TGF-β signaling activation [34], demonstrating PRMTs' involvement in epigenetic regulation of colorectal cancer. Additionally, PRMTs influence cancer progression by mediating critical signaling pathways controlling cell fate, including p53, EGFR, and Kelch-like ECH-associated protein 1 (KEAP1) signaling [35-37]. Liu *et al.* demonstrated that PRMT1 methylates cyclic GMP-AMP (cGas), suppressing cGas/stimulator of interferon genes (STING) signaling and facilitating immune surveillance evasion [38]. The role of PRMTs in cancer extends to immunotherapy and drug resistance [39, 40], potentially offering novel therapeutic strategies. In mammalian cells, PRMT1, a key type I PRMT, plays a crucial role in oncogenesis through protein arginine side chain methylation, making it a promising therapeutic target warranting extensive research.

Based on extensive research, PRMT1 has emerged as a promising target for addressing cancer MDR [30]. Takehiro et al. demonstrated that PRMT1 plays an essential role in maintaining de novo fatty acid synthesis through PHGDH methylation mediation, ultimately leading to chemoresistance in Triple-Negative breast cancer [41]. Xia-Lu and colleagues identified a positive feedback loop between PRMT1-mediated YAP methylation and methionine transporter SLC43A2, which contributes to anticancer drug resistance, emphasizing PRMT1's crucial role in cancer MDR [42]. However, the mechanisms of targeting PRMTs to address cancer MDR remain unclear due to the complexity of protein arginine methylation. In this study, we discovered that ABCB1-mediated MDR cancer cells, SW620/AD300 and KBV200 cells, exhibit significantly higher levels of EGFR methylation, particularly aDMA modulation, and stronger EGFR-PRMT1 interaction compared to their parental cells, SW620 and KB, indicating PRMT1 as a promising target for overcoming drug resistance. This research not only revealed PRMT1's involvement in cancer MDR progression but also demonstrated that TI, as a potent PRMT1 inhibitor, exhibited MDR reversal efficacy *in vivo* and *in vitro* through EGFR methylation impairment and EGFR signaling inhibition.

Previous research has established that PRMT1 activates EGFR signaling either through direct EGFR methylation catalysis or by inducing histone methylation on the EGFR promoter [28, 43]. Liao *et al.* demonstrated that PRMT1 enhances EGFR-ligand binding and receptor dimerization, along with subsequent signaling activation, by catalyzing R198/R200 methylation of the EGFR extracellular domain [28]. Consistently, our results show that TI reduced PRMT1 expression and induced a marked decrease in PRMT1-EGFR interaction, as well as subsequent aDMA modification of EGFR in SW620/AD300 and KBV200 cells. Additionally, p-EGFR, p-Akt, and p-Erk levels decreased with TI treatment, indicating EGFR signaling suppression. Notably, PRMT1 overexpression not only inhibited these TI activities in SW620/AD300 and KBV200 cells but also restored their drug resistance characteristics to chemotherapies, further confirming the crucial role of PRMT1-mediated aMDA of EGFR in TI-induced drug resistance reversal effect in ABCB1-overexpressing human cancer cells (Fig. 7).

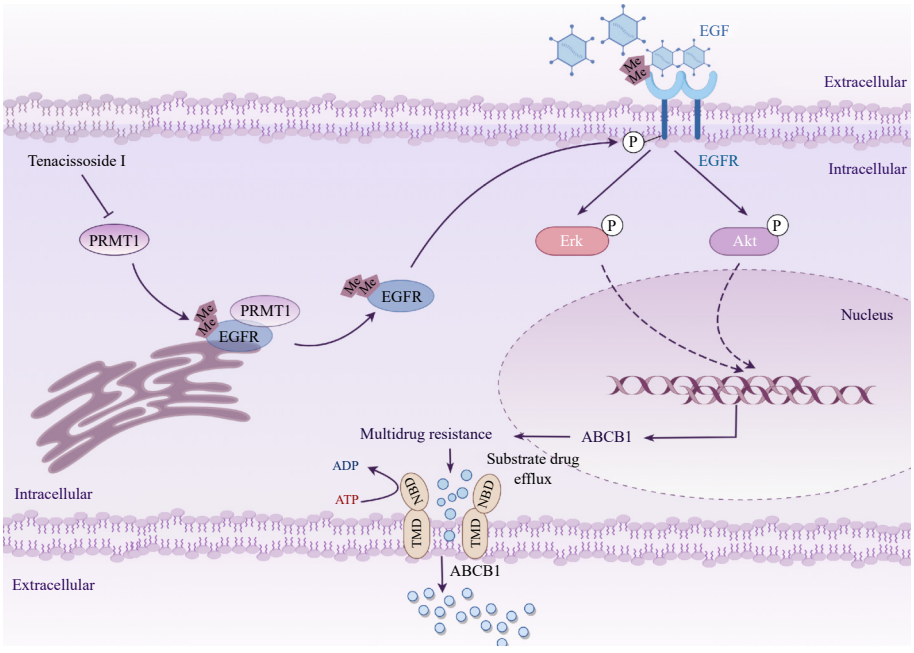

Fig. 7 Scheme illustrating TI's drug resistance reversal effect in ABCB1-mediated MDR cancer cells. (By Figdraw)

While we have elucidated TI's drug resistance reversal efficacy and its mechanism, several questions remain unresolved. For instance, our findings have only identified TI's reversal of ABCB1-mediated MDR, but not ABCG2-mediated MDR. A more comprehensive investigation is needed to verify this specificity of TI's MDR reversal effect. Additionally, the potential influence of TI on cancer MDR reversal through regulation of the cancer immune microenvironment requires examination. Furthermore, additional research into PRMT1's complex role in cancer MDR regulation, TI's specific mechanism in cancer management, and TI's poten-

tial targets in cancer MDR reversal remains essential. These questions warrant further investigation in future studies.

5. Conclusion

In conclusion, this study demonstrates that TI reverses ABCB1-mediated drug resistance in SW620/AD300 and KBV200 cells through PRMT1 downregulation, which mechanistically operates by demethylating EGFR and suppressing EGFR signaling. These findings highlight TI's potential as an MDR reversal candidate drug and provide insight into targeting PRMT1 as a strategy to overcome MDR in cancer management.

Funding

This work was supported by the National Natural Science Foundation of China (Nos. 82274211 and 82474190), the Natural Science Foundation of Tianjin (Nos. 24JCZDJC00120 and 24PTLYHZ00280), and Liaoning Provincial Department of Education Basic Research Projects for Higher Education Institutions (No. LJ212510163021).

Declaration of competing interest

These authors have no conflict of interest to declare.

References

1 Sung H, Ferlay J, Siegel RL, et al. Global Cancer Statistics 2020: GLOBOCAN estimates of incidence and mortality worldwide for 36 cancers in 185 countries. *CA Cancer J Clin*. 2021;71(3):209-249. https://doi.org/10.3322/caac.21660.
2 Yang C, Ding Y, Mao Z, et al. Nanoplatform-mediated autophagy regulation and combined anti-tumor therapy for resistant tumors. *Int J Nanomed*. 2024;19:917-944. https://doi.org/10.2147/ijn.S445578.
3 Shukla S, Chen ZS, Ambudkar SV. Tyrosine kinase inhibitors as modulators of ABC transporter-mediated drug resistance. *Drug Resist Updat*. 2012;15(1-2):70-80. https://doi.org/10.1016/j.drup.2012.01.005.
4 Szakács G, Paterson JK, Ludwig JA, et al. Targeting multidrug resistance in cancer. *Nat Rev Drug Discov*. 2006;5:219-234. https://doi.org/10.1038/nrd1984.
5 Saraswathy M, Gong S. Different strategies to overcome multidrug resistance in cancer. *Biotechnol Adv*. 2013;31(8):1397-1407. https://doi.org/10.1016/j.biotechadv.2013.06.004.
6 Gottesman MM, Fojo T, Bates SE. Multidrug resistance in cancer: role of ATP-dependent transporters. *Nat Rev Cancer*. 2002;2(1):48-58. https://doi.org/10.1038/nrc706.
7 Zhang H, Xu H, Jr Ashby CR, et al. Chemical molecular-based approach to overcome multidrug resistance in cancer by targeting P-glycoprotein (P-gp). *Med Res Rev*. 2021;41(1):525-555. https://doi.org/10.1002/med.21739.
8 Pan S, Chen R. Pathological implication of protein post-translational modifications in cancer. *Mol Aspects Med*. 2022;86:101097. https://doi.org/10.1016/j.mam.2022.101097.
9 Gao Y, Feng C, Ma J, et al. Protein arginine methyltransferases (PRMTs): Orchestrators of cancer pathogenesis, immunotherapy dynamics, and drug resistance. *Biochem Pharmacol*. 2024;221:116048. https://doi.org/10.1016/j.bcp.2024.116048.
10 El-Khoueiry AB, Clarke J, Neff T, et al. Phase 1 study of GSK3368715, a type I PRMT inhibitor, in patients with advanced solid tumors. *Br J Cancer*. 2023;129(2):309-317. https://doi.org/10.1038/s41416-023-02276-0.
11 Shen S, Zhou H, Xiao Z, et al. PRMT1 in human neoplasm: cancer biology and potential therapeutic target. *Cell Commun Signal*. 2024;22(1):102. https://doi.org/10.1186/s12964-024-01506-z.
12 Hwang JW, Cho Y, Bae GU, et al. Protein arginine methyltransferases: promising targets for cancer therapy. *Exp Mol Med*. 2021;53(5):788-808. https://doi.org/10.1038/s12276-021-00613-y.
13 Wang H, Huang ZQ, Xia L, et al. Methylation of histone H4 at arginine 3 facilitating transcriptional activation by nuclear hormone receptor. *Science*. 2001;293(5531):853-857. https://doi.org/10.1126/science.1060781.
14 Liu W, Wang Y, Xia L, et al. Research Progress of Plant-Derived Natural Products against Drug-Resistant Cancer. *Nutrients*. 2024;16(6):797. https://doi.org/10.3390/nu16060797.
15 Han SY, Zhao W, Sun H, et al. Marsdenia tenacissima extract enhances gefitinib efficacy in non-small cell lung cancer xenografts. *Phytomedicine*. 2015;22(5):560-567. https://doi.org/10.1016/j.phymed.2015.03.001.
16 Li X, He S, Liang W, et al. Marsdenia tenacissima injection induces the apoptosis of prostate cancer by regulating the AKT/GSK3β/STAT3 signaling axis. *Chin J Nat Med*. 2023;21(2):113-126. https://doi.org/10.1016/s1875-5364(23)60389-9.
17 Yao S, To KK, Wang YZ, et al. Polyoxypregnane steroids from the stems of *Marsdenia tenacissima*. *J Nat Prod*. 2014;77(9):2044-2053. https://doi.org/10.1021/np500385b.
18 Dong J, Qian Y, Zhang W, et al. Tenacissoside H repressed the progression of glioblastoma by inhibiting the PI3K/Akt/mTOR signaling pathway. *Eur J Pharmacol*. 2024;968:176401. https://doi.org/10.1016/j.ejphar.2024.176401.
19 Wang K, Liu W, Xu Q, et al. Tenacissoside G synergistically potentiates inhibitory effects of 5-fluorouracil to human colorectal cancer. *Phytomedicine*. 2021;86:153553. https://doi.org/10.1016/j.phymed.2021.153553.
20 Hu J, Hu Y, Zhang X, et al. Tenacissoside G reverses paclitaxel resistance by inhibiting Src/PTN/P-gp signaling axis activation in ovarian cancer cells. *J Nat Med*. 2025;79(3):621-638. https://doi.org/10.1007/s11418-025-01879-6.
21 Zhao C, Hao H, Zhao H, et al. Marsdenia tenacissima extract promotes gefitinib accumulation in tumor tissues of lung cancer xenograft mice via inhibiting ABCG2 activity. *J Ethnopharmacol*. 2020;255:112770. https://doi.org/10.1016/j.jep.2020.112770.
22 Zhao C, Han LY, Ren W, et al. Metabolic profiling of tenacigenin B, tenacissoside H and tenacissoside I using UHPLC-ESI-Orbitrap MS/MS. *Biomed Chromatogr*. 2016;30(11):1757-1765. https://doi.org/10.1002/bmc.3750.
23 Ji N, Li H, Zhang Y, et al. Lansoprazole (LPZ) reverses multidrug resistance (MDR) in cancer through impeding ATP-binding cassette (ABC) transporter-mediated chemotherapeutic drug efflux and lysosomal sequestration. *Drug Resist Updat*. 2024;76:101100. https://doi.org/10.1016/j.drup.2024.101100.
24 Ren Z, Su R, Liu D, et al. Yes-associated protein indispensably mediates hirsutine-induced inhibition on cell growth and Wnt/β-catenin signaling in colorectal cancer. *Phytomedicine*. 2024;135:156156. https://doi.org/10.1016/j.phymed.2024.156156.
25 Peng X, Huang X, Lulu TB, et al. A novel pan-PI3K inhibitor KTC1101 synergizes with anti-PD-1 therapy by targeting tumor suppression and immune activation. *Mol Cancer*. 2024;23(1):54. https://doi.org/10.1186/s12943-024-01978-0.
26 Peng X, Huang X, Zhang S, et al. Sequential inhibition of PARP and BET as a rational therapeutic strategy for glioblastoma. *Adv Sci (Weinh)*. 2024;11(30):e2307747. https://doi.org/10.1002/advs.202307747.
27 Wu Q, Schapira M, Arrowsmith CH, et al. Protein arginine methylation: from enigmatic functions to therapeutic targeting. *Nat Rev Drug Discov*. 2021;20(7):509-530. https://doi.org/10.1038/s41573-021-00159-8.
28 Liao HW, Hsu JM, Xia W, et al. PRMT1-mediated methylation of the EGF receptor regulates signaling and cetuximab response. *J Clin Invest*. 2015;125(12):4529-4543. https://doi.org/10.1172/jci82826.
29 Hu B, Zou T, Qin W, et al. Inhibition of EGFR overcomes acquired lenvatinib resistance driven by STAT3-ABCB1 signaling in hepatocellular carcinoma. *Cancer Res*. 2022;82(20):3845-3857. https://doi.org/10.1158/0008-5472.Can-21-4140.
30 Zhu Y, Xia T, Chen DQ, et al. Promising role of protein arginine methyltransferases in overcoming anti-cancer drug resistance. *Drug Resist Updat*. 2024;72:101016. https://doi.org/10.1016/j.drup.2023.101016.
31 Sun Y. Tumor microenvironment and cancer therapy resistance. *Cancer Lett*. 2016;380(1):205-215. https://doi.org/10.1016/j.canlet.2015.07.044.
32 Wu Q, Yang Z, Nie Y, et al. Multi-drug resistance in cancer chemotherapeutics: mechanisms and lab approaches. *Cancer Lett*. 2014;347(2):159-166. https://doi.org/10.1016/j.canlet.2014.03.013.
33 Lei Y, Han P, Tian D. Protein arginine methyltransferases and hepatocellular carcinoma: a review. *Transl Oncol*. 2021;14(11):101194. https://doi.org/10.1016/j.tranon.2021.101194.
34 Liu A, Yu C, Qiu C, et al. PRMT5 methylating SMAD4 activates TGF-β signaling and promotes colorectal cancer metastasis. *Oncogene*. 2023;42(19):1572-1584. https://doi.org/10.1038/s41388-023-02674-x.
35 Liu LM, Tang Q, Hu X, et al. Arginine methyltransferase PRMT1 regulates p53 activity in breast cancer. *Life (Basel)*. 2021;11(8):789. https://doi.org/10.3390/life11080789.
36 Ge L, Wang H, Xu X, et al. PRMT5 promotes epithelial-mesenchymal transition via EGFR-β-catenin axis in pancreatic cancer cells. *J Cell Mol Med*. 2020;24(2):1969-1979. https://doi.org/10.1111/jcmm.14894.
37 Wang Z, Li R, Hou N, et al. PRMT5 reduces immunotherapy efficacy in triple-negative breast cancer by methylating KEAP1 and inhibiting ferroptosis. *J Immunother Cancer*. 2023;11(6):e006890. https://doi.org/10.1136/jitc-2023-006890.
38 Liu J, Bu X, Chu C, et al. PRMT1 mediated methylation of cGAS suppresses anti-tumor immunity. *Nat Commun*. 2023;14(1):2806. https://doi.org/10.1038/s41467-023-38443-3.
39 Srour N, Villarreal OD, Hardikar S, et al. PRMT7 ablation stimulates anti-tumor immunity and sensitizes melanoma to immune checkpoint blockade. *Cell Rep*. 2022;38(13):110582. https://doi.org/10.1016/j.celrep.2022.110582.
40 Shi Y, Niu Y, Yuan Y, et al. PRMT3-mediated arginine methylation of IGF2BP1 promotes oxaliplatin resistance in liver cancer. *Nat Commun*. 2023;14(1):1932. https://doi.org/10.1038/s41467-023-37542-5.
41 Yamamoto T, Hayashida T, Masugi Y, et al. PRMT1 sustains *de novo* fatty acid synthesis by methylating PHGDH to drive chemoresistance in triple-negative breast cancer. *Cancer Res*. 2024;84(7):1065-1083. https://doi.org/10.1158/0008-5472.Can-23-2266.
42 Hong XL, Huang CK, Qian H, et al. Positive feedback between arginine methylation of YAP and methionine transporter SLC43A2 drives anticancer drug resistance. *Nat Commun*. 2025;16(1):87. https://doi.org/10.1038/s41467-024-55769-8.
43 Yao B, Gui T, Zeng X, et al. PRMT1-mediated H4R3me2a recruits SMARCA4 to promote colorectal cancer progression by enhancing EGFR signaling. *Genome Med*. 2021;13(1):58. https://doi.org/10.1186/s13073-021-00871-5.